Performance Evaluation of a Viterbi Detector in the Presence of Correlated Noise

Yasutaka OGAWA* Masakazu SENGOKU Tadashi MATSUMOTO***

(Received June 22, 1978)

Abstract

Viterbi algorithm detection is of considerable interest for high-speed data transmission over a voiceband telephone channel. This paper describes the effect of noise correlation on a data communication system which employs a Viterbi detector. First, a new evaluation function is introduced in order to observe performance characteristics of a Viterbi detector. And it is shown that the lower bound of the evaluation function is expressed in terms of the equivalent Nyquist power spectrum of a noise component. Moreover, numerical calculations were made for single-sideband systems with data rates of 10,000 bits/s and 12,000 bits/s.

1. Introduction

Recently, Viterbi algorithm detection has been studied extensively for the purpose of implementing a high-speed data transmission system over a voiceband telephone channel[1)~7),11)]. However, the number of computations per symbol performed by a Viterbi detector grows exponentially with the length of a desired impulse response[3)] (abbreviated as DIR). In order to simplify the implementation of the Viterbi detector, a receiver filter placed in front of the Viterbi detector must be adjusted in such a way that the length of the DIR is acceptably short. Because the adjusted receiver filter is generally different from a whitened matched filter[1)], the noise component at the input to the Viterbi detector is correlated. It should be noted that even if the channel noise is white, the noise component at the input to the Viterbi detector is colored by the receiver filter.

On the other hand, an effective signal-to-noise ratio is commonly used for the performance evaluation of a Viterbi detector. The effective signal-to-noise ratio is calculated by means of the minimum distance of an error event and the noise variance which does not depend on an error event[1)]. However, as stated in Section 3, if the noise component is correlated, the distribution of the noise component depends on an error event. Consequently, the conventional effective signal-to-noise ratio is not an adequate evaluation function when the noise component is correlated. Qureshi and Newhall have considered the performance of a Viterbi detector in the presence of correlated noise[2)]. Unfortunately, they did not show

* Department of Electronics Engineering, Faculty of Engineering, Hokkaido University, Sapporo, 060, Japan.

** Department of Information Engineering, Faculty of Engineering, Niigata University, Nagaoka, 940, Japan.

the general method of performance evaluation, but they only solved a simple exaample. And their results are not sufficient to evaluate the performance of a factual data communication system with a Viterbi detector. Accordingly, it may be said that a systematic study has not been done on the correlated noise problem.

This paper deals with the effect of noise correlation on a communication system which employs a Viterbi detector. In Section 2, a new evaluation function is defined which is interpreted as the extention of the conventional effective signal-to-noise ratio. Then, in Section 3, a new concept, called an equivalent Nyquist power spectrum of the noise component, is introduced. And the lower bound of the evaluation function is derived analytically by using the equivalent Nyquist power spectrum. Finally, in Section 4, numerical results are shown. The numerical calculations were made for single-sideband amplitude modulation systems with data rates of 10,000 bits/s and 12,000 bits/s.

2. Notation and Basic Definitions

In a high-speed data transmission system over a voiceband telephone channel, amplitude modulation and synchronous demodulation are employed in order to use a channel passband efficiently. In this case a carrier transmission system is transformed into an equivalent digital PAM baseband model by means of simple calculations[10]. Accordingly, it is possible to discuss our problem by using the equivalent baseband model shown in Fig. 1.

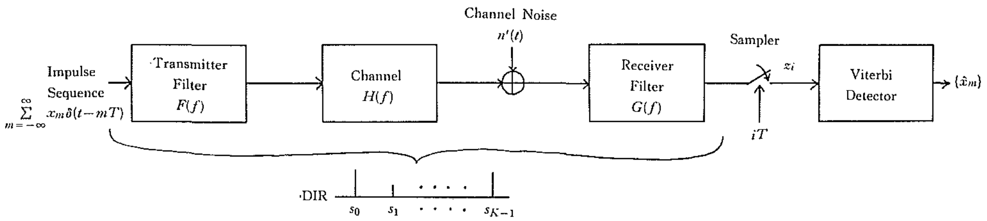

Fig. 1. Equivalent digital PAM baseband model.

Necessary symbols are defined as follows.

$F(f)$: Frequency characteristic of the transmitter filter

$H(f)$: Frequency characteristic of the equivalent baseband channel

$G(f)$: Frequency characteristic of the receiver filter

$g(t)$: Impulse response of the receiver filter

T : Signaling interval

$\{s_i\}_{i=0}^{K-1}$: DIR (an overall sampled impulse response of the communication system seen by the Viterbi detector)

The Viterbi detector makes decisions on the assumption that the DIR $\{s_i\}_{i=0}^{K-1}$ is the actual overall system response. Here, we express the length of the DIR as K. Thus, we obtain

$$s_i = 0 \quad \text{for} \quad i<0 \quad \text{or} \quad i \geqq K \tag{1}$$

$$s_0 s_{K-1} \neq 0\,. \tag{2}$$

x_m : Message transmitted at time mT
Each x_m is assumed to take on the values $(M-1)/2$, $(M-3)/2, \cdots$, $(1-M)/2$ with equal probability. It is also assumed that the sequence $\{x_m\}_{m=-\infty}^{\infty}$ is a white stationary stochastic process with variance σ_x^2. Thus, we have

$$\sigma_x^2 \triangleq E\{x_m^2\} \\ =(M^2-1)/12 \tag{3}$$

where $E\{\cdot\}$ denotes ensemble average.
We consider that an impulse sequence $\sum_{m=-\infty}^{\infty} x_m \delta(t-mT)$ is transmitted to the channel $H(f)$ over the transmitter filter $F(f)$.

$\hat{x}_m$: Estimated value of x_m decided upon by the Viterbi detector

$\{\varepsilon_{xj}\}_{j=1}^{N}$: Input error sequence associated with an error event[1] ε
Each component ε_{xj} is defined as follows. Let the error event ε have the following relation between $\{x_i\}_{i=-\infty}^{\infty}$ and $\{\hat{x}_i\}_{i=-\infty}^{\infty}$.

$$x_i = \hat{x}_i \qquad \text{for } i \leqq l \text{ or } i > l+N \ (N>0) \tag{4}$$

$$x_{l+1} \neq \hat{x}_{l+1} \quad \text{and} \quad x_{l+N} \neq \hat{x}_{l+N} \tag{5}$$

Here, N is called a length of the error event ε. Then, we define ε_{xj} as

$$\varepsilon_{xj} \triangleq x_{l+j} - \hat{x}_{l+j} \qquad (1 \leqq j \leqq N)\,. \tag{6}$$

We consider all error events with the same input error sequence $\{\varepsilon_{xj}\}_{j=1}^{N}$ to be identical.

$\{\varepsilon_{yj}\}_{j=1}^{N+K-1}$: Signal error sequence associated with the error event ε
Each component ε_{yj} is defined as

$$\varepsilon_{yj} \triangleq \sum_{i=0}^{K-1} \varepsilon_{xj-i} s_i \qquad \text{for} \quad 1 \leqq j \leqq N+K-1 \tag{7}$$

where

$$\varepsilon_{xj} = 0 \qquad \text{for} \quad j<0 \quad \text{or} \quad j>N\,. \tag{8}$$

Moreover, we define a signal error vector $\boldsymbol{\varepsilon}_y(\varepsilon)$ associated with the error event ε as

$$\boldsymbol{\varepsilon}_y(\varepsilon) \triangleq [\varepsilon_{y1}\, \varepsilon_{y2} \cdots \varepsilon_{yN+K-1}]^T \tag{9}$$

where $[\cdots]^T$ stands for a matrix transposed.
As can be seen from Eq. (9), $\boldsymbol{\varepsilon}_y(\varepsilon)$ has $(N+K-1)$ rows.

$d(\varepsilon)$: Euclidean norm associated with the error event ε
$d(\varepsilon)$ is defined as

$$d(\varepsilon) \triangleq \sqrt{\sum_{i=0}^{N+K-1} \varepsilon_{yi}^2}\,. \tag{10}$$

$n'(t)$: Channel noise
$n'(t)$ is assumed to be a 0-mean stationary stochastic process with a power spectrum density $N_0/2$. And $n'(t)$ is also assumed to be statistically independent of $\{x_m\}_{m=-\infty}^{\infty}$.

z_i : Input value to the Viterbi detector at time iT
Using the above symbols, z_i is expressed as

$$\begin{aligned} z_i = &\sum_{n=-\infty}^{\infty} x_n \int_{-1/2T}^{1/2T} \big[F(f)\,H(f)\,G(f)\big]_{eq} e^{j2\pi f(i-n)T} df \\ &+ \int_{-\infty}^{\infty} n'(\tau)\, g(iT-\tau)\, d\tau \end{aligned} \tag{11}$$

where $[X(f)]_{eq}$ represents an equivalent Nyquist channel characteristic[10] defined as

$$\big[X(f)\big]_{eq} \triangleq \begin{cases} \sum_{l=-\infty}^{\infty} X(f+l/T) & \text{for } |f| \leqq 1/2T \\ 0 & \text{for } |f| > 1/2T\,. \end{cases} \tag{12}$$

n_i : Noise component at the input to the Viterbi detector at time iT
n_i is defined as

$$n_i \triangleq z_i - \sum_{j=0}^{K-1} s_j x_{i-j}\,. \tag{13}$$

Substituting Eq. (11) into Eq. (13), we obtain

$$n_i = n_i^{(1)} + n_i^{(2)} \tag{14}$$

where

$$\begin{aligned} n_i^{(1)} \triangleq \sum_{n=-\infty}^{\infty} x_n \int_{-1/2T}^{1/2T} \Big\{ &\big[F(f)\,H(f)\,G(f)\big]_{eq} \\ &- \big[S(f)\big]_{eq} \Big\} e^{j2\pi f(i-n)T} df \end{aligned} \tag{15}$$

$$\big[S(f)\big]_{eq} \triangleq \begin{cases} T \sum_{l=0}^{K-1} s_l e^{-j2\pi f l T} & \text{for } |f| \leqq 1/2T \\ 0 & \text{for } |f| > 1/2T \end{cases} \tag{16}$$

$$n_i^{(2)} \triangleq \int_{-\infty}^{\infty} n'(\tau)\, g(iT-\tau)\, d\tau\,. \tag{17}$$

Here, $n_i^{(1)}$ is interpreted as the vestigial error component which arises because the DIR is not exactly equivalent to the actual sampled impulse response of the system. And $n_i^{(2)}$ is the filtered channel noise. The sequence $\{n_i\}_{i=-\infty}^{\infty}$ is a 0-mean stationary stochastic process. Here, we define an autocorrelation sequence of $\{n_i\}_{i=-\infty}^{\infty}$ as $\{\rho_l\}_{l=-\infty}^{\infty}$, i. e.,

$$\rho_l \triangleq E\{n_0 n_l\}\,. \tag{18}$$

The variance of $\{n_i\}_{i=-\infty}^{\infty}$ is represented by σ_n^2, i. e.,

$$\sigma_n^2 \triangleq E\{n_0^2\}. \tag{19}$$

We define a noise vector $\boldsymbol{n}_{l+1}^{l+N+K-1}$ as

$$\boldsymbol{n}_{l+1}^{l+N+K-1} \triangleq [n_{l+1}\ n_{l+2}\ \cdots\ n_{l+N+K-1}]^T. \tag{20}$$

Furthermore, we represent a norm of orthogonal projection of $\boldsymbol{n}_{l+1}^{l+N+K-1}$ on $\boldsymbol{\varepsilon}_y(\varepsilon)$ by $\tilde{n}(\varepsilon)_{l+1}^{l+N+K-1}$. (Fig. 2) Thus, $\tilde{n}(\varepsilon)_{l+1}^{l+N+K-1}$ is expressed as

$$\tilde{n}(\varepsilon)_{l+1}^{l+N+K-1} = \frac{|\boldsymbol{\varepsilon}_y(\varepsilon)^T \boldsymbol{n}_{l+1}^{l+N+K-1}|}{\sqrt{\boldsymbol{\varepsilon}_y(\varepsilon)^T \boldsymbol{\varepsilon}_y(\varepsilon)}}. \tag{21}$$

The variance of $\tilde{n}(\varepsilon)_{l+1}^{l+N+K-1}$ is represented by $\sigma_n(\varepsilon)^2$, i. e.,

$$\sigma_n(\varepsilon)^2 \triangleq E\left\{\left(\tilde{n}(\varepsilon)_{l+1}^{l+N+K-1}\right)^2\right\}. \tag{22}$$

Note that $\sigma_n(\varepsilon)^2$ does not depend on l since $\{n_i\}_{i=-\infty}^{\infty}$ is stationary.

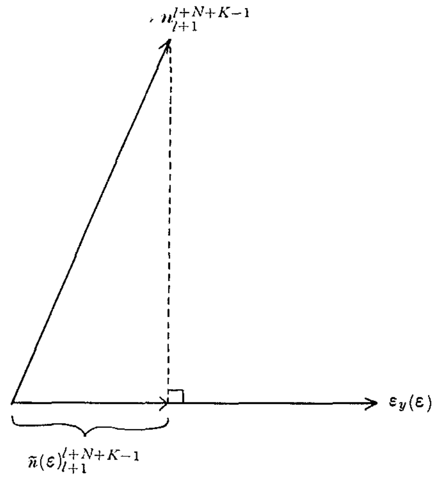

Fig. 2. Orthogonal projection of $\boldsymbol{n}_{l+1}^{l+N+K-1}$ on $\boldsymbol{\varepsilon}_y(\varepsilon)$.

$ESN^{(K)}$: Effective signal-to-noise ratio
$ESN^{(K)}$ is defined as

$$ESN^{(K)} \triangleq \sigma_x^2 \min_{\varepsilon} \frac{d(\varepsilon)^2}{\sigma_n{}^2}. \tag{23}$$

Note that K represents the length of the DIR as mentioned previously.

$ESN_c^{(K)}$: Effective signal-to-noise ratio which takes noise correlation into account
$ESN_c^{(K)}$ is defined as

$$ESN_c^{(K)} \triangleq \sigma_x^2 \min_{\varepsilon} \frac{d(\varepsilon)^2}{\sigma_n(\varepsilon)^2}. \tag{24}$$

In a case where the noise component n_i is (colored) Gaussian noise, the symbol error probability $Pr(E)$ is dominated at a moderate signal-to-noise ratio by the term imvolving $ESN_c^{(K)}$, i. e.,

$$Pr(E) \simeq K_e Q\left(\frac{1}{2}\sqrt{\frac{1}{\sigma_x^2} ESN_c^{(K)}}\right) \tag{25}$$

where K_e is a constant depending on the error event ε which minimizes $d(\varepsilon)^2/\sigma_n(\varepsilon)^2$. And $Q(w)$ is defined as

$$Q(w) \triangleq \frac{1}{\sqrt{2\pi}} \int_w^\infty e^{-\frac{u^2}{2}} du . \tag{26}$$

As can be seen from the expression (25), the greater $ESN_c^{(K)}$ is, a tendency for a smaller symbol error probability $Pr(E)$ is seen. Even if the noise component n_i is not Gaussian noise, $ESN_c^{(K)}$ is considered to be an adequate evaluation function. The reason for this is that $ESN_c^{(K)}$ takes into account both noise correlation and the Euclidean norm associated with an error event. Therefore, we will use $ESN_c^{(K)}$ for a performance evaluation function of the Viterbi detector.

3. Derivation of Lower Bound of $ESN_c^{(K)}$

Although the new evaluation function $ESN_c^{(K)}$ is introduced in the previous section, it is impossible to calculate $ESN_c^{(K)}$ analytically. The reason for this is that there is no analytical way to obtain the error event ε which minimizes $d(\varepsilon)^2/\sigma_n(\varepsilon)^2$. Accordingly, we derive a lower bound of $ESN_c^{(K)}$ for performance evaluation. First, we show the following Lemma 1.

Lemma 1

Each ρ_l is given by the following equation.

$$\rho_l = \int_{-\infty}^{\infty} \left[P(f)\right]_{eq} e^{j2\pi f l T} df \tag{27}$$

where

$$\left[P(f)\right]_{eq} \triangleq \begin{cases} \frac{\sigma_x^2}{T}\left|\left[F(f)\,H(f)\,G(f)\right]_{eq} - \left[S(f)\right]_{eq}\right|^2 + \frac{N_0}{2}\left[|G(f)|^2\right]_{eq} & \text{for } |f| \leqq 1/2T \\ 0 & \text{for } |f| > 1/2T . \end{cases} \tag{28}$$

Proof

Because $n'(t)$ is statistically independent of $\{x_m\}_{m=-\infty}^{\infty}$, the stochastic processes of $\{n_i^{(1)}\}_{i=-\infty}^{\infty}$ and $\{n_i^{(2)}\}_{i=-\infty}^{\infty}$ are statistically independent of each other. Therefore, we obtain

$$\begin{aligned} \rho_l &= E\left\{(n_0^{(1)} + n_0^{(2)})\,(n_l^{(1)} + n_l^{(2)})\right\} \\ &= \rho_l^{(1)} + \rho_l^{(2)} \end{aligned} \tag{29}$$

where

$$\rho_l^{(1)} \triangleq E\{n_0^{(1)} n_l^{(1)}\} \tag{30}$$

$$\rho_l^{(2)} \triangleq E\{n_0^{(2)} n_l^{(2)}\} . \tag{31}$$

Substituting Eq. (15) into Eq. (30) and using the statistical properties of $\{x_m\}_{m=-\infty}^{\infty}$, $\rho_l^{(1)}$ is expressed as

$$\begin{aligned}\rho_l^{(1)} = \sigma_x^2 \int_{-1/2T}^{1/2T} \int_{-1/2T}^{1/2T} &\Big\{\big[F(f_1)\, H(f_1)\, G(f_1)\big]_{eq} - \big[S(f_1)\big]_{eq}\Big\} \\ &\times \Big\{\big[F(f_2)\, H(f_2)\, G(f_2)\big]_{eq} - \big[S(f_2)\big]_{eq}\Big\} e^{j2\pi f_2 lT} \\ &\times \sum_{n=-\infty}^{\infty} e^{-j2\pi(f_1+f_2)nT} df_1 df_2 .\end{aligned} \tag{32}$$

Furthermore, by using

$$\sum_{n=-\infty}^{\infty} e^{-j2\pi f nT} = \frac{1}{T} \sum_{m=-\infty}^{\infty} \delta\left(f - \frac{m}{T}\right) \tag{33}$$

Eq. (32) becomes

$$\rho_l^{(1)} = \frac{\sigma_x^2}{T} \int_{-1/2T}^{1/2T} \Big|\big[F(f)\, H(f)\, G(f)\big]_{eq} - \big[S(f)\big]_{eq}\Big|^2 e^{j2\pi f lT} df . \tag{34}$$

From Eq. (17), $\rho_l^{(2)}$ is expressed as

$$\rho_l^{(2)} = \frac{N_0}{2} \int_{-\infty}^{\infty} \big|G(f)\big|^2 e^{j2\pi f lT} df . \tag{35}$$

From Eq. (35), it is easily seen that $\rho_l^{(2)}$ is given by

$$\rho_l^{(2)} = \frac{N_0}{2} \int_{-1/2T}^{1/2T} \Big[\big|G(f)\big|^2\Big]_{eq} e^{j2\pi f lT} df . \tag{36}$$

Substituting Eq. (34) and Eq. (36) into Eq. (29), we obtain Eq. (27). (Q. E. D.)

The Lemma 1 tells us that the sampled inverse Fourier transform of $[P(f)]_{eq}$ is equivalent to ρ_l which is the autocorrelation sequence of $\{n_i\}_{i=-\infty}^{\infty}$. And the band of $[P(f)]_{eq}$ is circumscribed within the Nyquist-band ($|f| \leqq 1/2T$). Thus, we refer to $[P(f)]_{eq}$ as the equivalent Nyquist power spectrum of the noise component $\{n_i\}_{i=-\infty}^{\infty}$.

Then, we show the following Lemma 2.

Lemma 2

For an arbitary error event ε, $\sigma_n(\varepsilon)^2$ is upperbounded by

$$\sigma_n(\varepsilon)^2 \leqq \frac{1}{T} \max_{\substack{f \\ (|f| \leqq 1/2T)}} \big[P(f)\big]_{eq} . \tag{37}$$

Proof

Let the error event ε have the length $J-K+1$. Substituting Eq. (21) into Eq. (22), we obtain

$$\begin{aligned}\sigma_n(\varepsilon)^2 &= \frac{\boldsymbol{\varepsilon}_y(\varepsilon)^T E\{(\boldsymbol{n}_{l+1}^{l+J})(\boldsymbol{n}_{l+1}^{l+J})^T\}\,\boldsymbol{\varepsilon}_y(\varepsilon)}{\boldsymbol{\varepsilon}_y(\varepsilon)^T\boldsymbol{\varepsilon}_y(\varepsilon)} \\ &= \frac{\boldsymbol{\varepsilon}_y(\varepsilon)^T \Phi^{(J)}\,\boldsymbol{\varepsilon}_y(\varepsilon)}{\boldsymbol{\varepsilon}_y(\varepsilon)^T\boldsymbol{\varepsilon}_y(\varepsilon)}\end{aligned} \tag{38}$$

where $\boldsymbol{\varepsilon}_y(\varepsilon)$ is a column vector of dimension J and

$$\Phi^{(J)} \triangleq E\left\{(\boldsymbol{n}_{l+1}^{l+J})(\boldsymbol{n}_{l+1}^{l+J})^T\right\} \tag{39}$$

is a $J\times J$ covariance matrix of the noise component $\{n_i\}_{i=-\infty}^{\infty}$. From Eq. (18) and Eq. (39), it is seen that $\Phi^{(J)}$ is a symmetric Toeplitz matrix whose element ϕ_{ij} is expressed as

$$\phi_{ij} = \rho_{|i-j|} \tag{40}$$

Thus, $\Phi^{(J)}$ is written as

$$\Phi^{(J)} = \begin{pmatrix} \rho_0 & \rho_1 & \rho_2 & \cdots & \rho_{J-1} \\ \rho_1 & \rho_0 & \rho_1 & \cdots & \rho_{J-2} \\ \rho_2 & \rho_1 & \rho_0 & \ddots & \vdots \\ \vdots & \vdots & \ddots & \ddots & \rho_1 \\ \rho_{J-1} & \rho_{J-2} & \rho_{J-3} \cdots & \rho_1 & \rho_0 \end{pmatrix}. \tag{41}$$

Let $\boldsymbol{v}_J$ be an arbitary real and column vector of dimension J. Then, the following inequality holds.

$$\max_{\boldsymbol{\varepsilon}_y(\varepsilon)} \frac{\boldsymbol{\varepsilon}_y(\varepsilon)^T\Phi^{(J)}\boldsymbol{\varepsilon}_y(\varepsilon)}{\boldsymbol{\varepsilon}_y(\varepsilon)^T\boldsymbol{\varepsilon}_y(\varepsilon)} \leqq \max_{\boldsymbol{v}_J}\frac{\boldsymbol{v}_J{}^T\Phi^{(J)}\boldsymbol{v}_J}{\boldsymbol{v}_J{}^T\boldsymbol{v}_J} \tag{42}$$

Now, we express the maximum eigen value of $\Phi^{(J)}$ as $\lambda_{\max}^{(J)}$. Then, we obtain

$$\max_{\boldsymbol{v}_J}\frac{\boldsymbol{v}_J{}^T\Phi^{(J)}\boldsymbol{v}_J}{\boldsymbol{v}_J{}^T\boldsymbol{v}_J} = \lambda_{\max}^{(J)}. \tag{43}$$

By using the Sturmian separation theorem[8], the inequality

$$\lambda_{\max}^{(J)} \leqq \lambda_{\max}^{(J+1)} \tag{44}$$

is obtained. Note that $\lambda_{\max}^{(J+1)}$ is the maximum eigen value of $\Phi^{(J+1)}$. Thus,

$$\max_J \lambda_{\max}^{(J)} = \lim_{J\to\infty}\lambda_{\max}^{(J)}. \tag{45}$$

Here, we define the Laurent series $\zeta_J(z)$ as

$$\zeta_J(z) \triangleq \rho_0 + \sum_{l=1}^{J-1}\rho_l(z^l+z^{-l}). \tag{46}$$

From properties of a symmetric Toeplitz matrix, $\lim\limits_{J\to\infty}\lambda_{\max}^{(J)}$ is equivalent to the maximum value of the Laurent series $\lim\limits_{J\to\infty}\zeta_J(z)$ under the constraint that z is on the unit circle[9], i. e.,

$$\lim_{J\to\infty} \lambda_{\max}^{(J)} = \max_{\substack{z\\(|z|=1)}} \left\{ \rho_0 + \sum_{l=1}^{\infty} \rho_l (z^l + z^{-l}) \right\}. \tag{47}$$

Then, we set z equal to $e^{j2\pi fT}$, i. e.,

$$z = e^{j2\pi fT} \qquad \text{for } |f| \leqq 1/2T. \tag{48}$$

Substituting Eq. (48) into Eq. (47), we have

$$\lim_{J\to\infty} \lambda_{\max}^{(J)} = \max_{\substack{f\\(|f|\leqq 1/2T)}} \left\{ \rho_0 + 2\sum_{l=1}^{\infty} \rho_l \cos 2\pi f l T \right\}. \tag{49}$$

Furthermore, by using expressions (38), (42), (43), (45) and (49), we get

$$\max_{\varepsilon} \sigma_n(\varepsilon)^2 \leqq \max_{\substack{f\\(|f|\leqq 1/2T)}} \left\{ \rho_0 + 2\sum_{l=1}^{\infty} \rho_l \cos 2\pi f l T \right\}. \tag{50}$$

From Eq. (28), Eq. (27) becomes

$$\rho_l = \int_{-1/2T}^{1/2T} \Big[P(f)\Big]_{eq} e^{j2\pi f l T} df. \tag{51}$$

Eq. (51) tells us that $T\rho_l$ is a Fourier coefficient of $[P(f)]_{eq}$. Since $[P(f)]_{eq}$ is an even function for $|f| \leqq 1/2T$, we obtain

$$\rho_0 + 2\sum_{l=1}^{\infty} \rho_l \cos 2\pi f l T = \frac{1}{T}\Big[P(f)\Big]_{eq} \qquad \text{for } |f| \leqq 1/2T. \tag{52}$$

Substituting Eq. (52) into the inequality (50), we obtain the inequality (37). (Q. E. D.)

Now, we show that the lower bound of $ESN_c^{(K)}$ is calculated by means of the equivalent Nyquist power spectrum ($[P(f)]_{eq}$) of the noise component.

Theorem 1

The lower bound of $ESN_c^{(K)}$ is given by

$$ESN_c^{(K)} \geqq \frac{\sigma_x^2 d_{\min}^2}{\dfrac{1}{T} \max\limits_{\substack{f\\(|f|\leqq 1/2T)}} \Big[P(f)\Big]_{eq}} \tag{53}$$

where

$$d_{\min} = \min_{\varepsilon} d(\varepsilon). \tag{54}$$

Proof

The proof of this theorem is quite easy. From the definition of $ESN_c^{(K)}$ (Eq. (24)),

$$ESN_c^{(K)} \geqq \sigma_x^2 \frac{\min\limits_{\varepsilon} d(\varepsilon)^2}{\max\limits_{\varepsilon} \sigma_n(\varepsilon)^2} \tag{55}$$

is obtained. Then, using Lemma 2 and Eq. (54), we get

$$\frac{\min\limits_{\varepsilon} d(\varepsilon)^2}{\max\limits_{\varepsilon} \sigma_n(\varepsilon)^2} \geqq \frac{d_{\min}^2}{\frac{1}{T} \max\limits_{\substack{f \\ (|f| \leqq 1/2T)}} \left[P(f)\right]_{eq}} . \tag{56}$$

From the inequality (55) and (56), it is seen that the inequality (53) holds. (Q. E. D.)

Using Theorem 1, the following corollary is obtained.

Corollary 1

When a receiver filter $G(f)$ is adjusted in such a way that the variance σ_n^2 defined by Eq. (19) is minimized for the given DIR, the lower bound of $ESN_c^{(K)}$ is given by

$$ESN_c^{(K)} \geqq \frac{\sigma_x^2 d_{\min}^2}{\max\limits_{\substack{f \\ (|f| \leqq 1/2T)}} \dfrac{\frac{N_0}{2T^2} \left| \left[S(f)\right]_{eq} \right|^2}{\frac{1}{T}\left[|F(f)\, H(f)|^2\right]_{eq} + \frac{N_0}{2\sigma_x^2}}} . \tag{57}$$

Proof

The optimum receiver filter structure is a matched filter followed by an infinite-length tapped delay line[3]. And the frequency characteristic of the optimum receiver filter is given by

$$G(f) = \frac{TF(f)^*\, H(f)^* \sum\limits_{n=0}^{K-1} s_n e^{-j2\pi f nT}}{\sum\limits_{n=-\infty}^{\infty} \left| F\!\left(f+\frac{n}{T}\right) H\!\left(f+\frac{n}{T}\right) \right|^2 + \frac{N_0 T}{2\sigma_x^2}} , \tag{58}$$

where * indicates a conjugate complex number. Substituting Eq. (58) into Eq. (28) and using Theorem 1, inequality (57) is derived. (Q. E. D.)

4. Numerical Results

In order to observe the performance, we made numerical calculations for communication system with data rates of 10,000 bits/s and 12,000 bits/s. The calculations were made under the following conditions and assumptions.

1) SSB-AM (single-sideband amplitude modulation) is employed for the efficient use of the transmission band. And the lower sideband is transmitted to the channel. On the other hand, the baseband signal is regenerated by means of synchronous demodulation. And it is assumed that carrier recovery and timing recovery are performed perfectly at the receiver.

2) The parameters of the transmitted signals are shown below.

(A) 10,000 bits/s system

- Carrier frequency 2,900 Hz
- Baud rate ($1/T_A$) 5,000 Baud
- M (The number which each x_m may take.) 4
- Transmitted wave shape Class 4 partial response, i. e.,

$$F(f)=\begin{cases} j\frac{6}{5}\sin 2\pi fT_A & \text{for } |f|\leqq 1/2T_A \\ 0 & \text{for } |f|>1/2T_A \end{cases} \tag{59}$$

(B) 12,000 bits/s system

- Carrier frequency 3,300 Hz
- Baud rate ($1/T_B$) 6,000 Baud
- M 4
- Transmitted wave shape Class 4 partial response, i. e.,

$$F(f)=\begin{cases} j\sin 2\pi fT_B & \text{for } |f|\leqq 1/2T_B \\ 0 & \text{for } |f|>1/2T_B \end{cases} \tag{60}$$

Note that transmitted wave shape of the 10,000 bits/s system is normalized in such a way that this system has the same transmitted power as the 12,000 bits/s system.

3) The frequency characteristics of the channel are shown in Fig. 3 and Fig. 4. Both are voiceband telephone channels. We consider that Channel 2 is a bad channel due to a very narrow and not very flat passband.

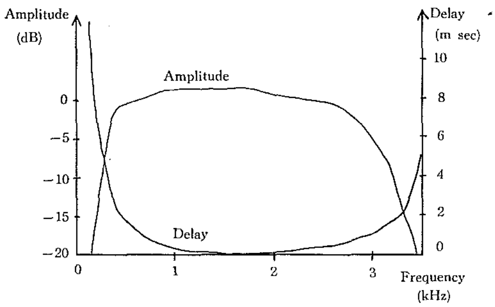

Fig. 3. Frequency characteristic of Channel 1.

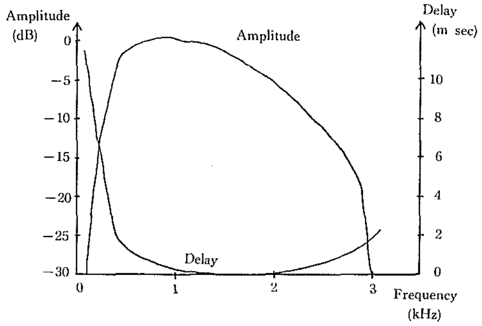

Fig. 4. Frequency characteristic of Channel 2.

4) The power spectrum density of channel noise ($N_0/2$) is determined in such a way that the following equation holds.

$$\frac{\sigma_x^2}{T_B}\int_{-\infty}^{\infty}\left|F(f)\,H(f)\right|^2 df \Big/ \frac{N_0}{2T_B}=10^3 \tag{61}$$

where $T_B=1/6000$ and $F(f)$ is given by Eq. (60). The physical meaning of Eq. (61) is that in the 12,000 bits/s system the ratio of the signal power in the channel $\left(\frac{\sigma_x^2}{T_B}\int_{-\infty}^{\infty}\left|F(f)\,H(f)\right|^2 df\right)$ to the noise power in the Nyquist-band ($N_0/2T_B$) equals 30 dB.

5) Filtering at the receiver is not done to the passband signal, but is done to the baseband signal. The receiver filter ($G(f)$) and the DIR are determined in such a way that the conventional effective signal-to-noise ratio ($ESN^{(K)}$) is maximized[11]. In this case the lower bound of $ESN_c^{(K)}$ is given by the Corollary 1.

The numerical results are shown in Table I through Table IV. Although the conventional effective signal-to-noise ratio ($ESN^{(K)}$) is also listed in those tables, it should be noted that $ESN_c^{(K)}$ is a better evaluation function than $ESN^{(K)}$.

As stated previously, the receiver filter and the DIR are not optimized with

TABLE 1. 10,000 bits/s results on Channel 1

K	DIR	$\{\varepsilon_{xj}\}_{j=1}^{N}$ which gives $d_{\min}$	Lower bound of $ESN_c^{(K)}$ (dB)	$ESN^{(K)}$ (dB)
2	{1, −1}	{1}	−3.0	16.4
3	{1, 0, −1}	{1}	27.8	30.5
4	{1, −1, −1, 1}	{1} & {1, 1, 2, 2, 3, 3, 3, 2, 2, 1, 1}	26.9	31.0

TABLE 2. 10,000 bits/s results on Channel 2

K	DIR	$\{\varepsilon_{xj}\}_{j=1}^{N}$ which gives $d_{\min}$	Lower bound of $ESN_c^{(K)}$ (dB)	$ESN^{(K)}$ (dB)
2	{1, −1}	{1}	−3.0	17.5
3	{1, 0, −1}	{1}	19.3	26.2
4	{1, −1, −1, 1}	{1} & {1, 1, 2, 2, 3, 3, 3, 2, 2, 1, 1}	29.3	31.7

TABLE 3. 12,000 bits/s results on Channel 1

K	DIR	$\{\varepsilon_{xj}\}_{j=1}^{N}$ which gives $d_{\min}$	Lower bound of $ESN_c^{(K)}$ (dB)	$ESN^{(K)}$ (dB)
2	{1, −1}	{1}	−3.0	15.1
3	{1, 0, −1}	{1}	21.0	27.9
4	{1, −1, −1, 1}	{1} & {1, 1, 2, 2, 3, 3, 3, 2, 2, 1, 1}	24.9	29.9

TABLE 4. 12,000 bits/s results on Channel 2

K	DIR	$\{\varepsilon_{xj}\}_{j=1}^{N}$ which gives $d_{\min}$	Lower bound of $ESN_c^{(K)}$ (dB)	$ESN^{(K)}$ (dB)
2	{1, −1}	{1}	−3.0	15.4
3	{1, 0, −1}	{1}	8.6	19.4
4	{1.0148, −0.985, −0.985, 1.0148}	{1, 1, 2, 2, 3, 3, 3, 2, 2, 1, 1}	24.2	28.3

respect to $ESN_c^{(K)}$, but they are determined in such a way that they maximize $ESN^{(K)}$. Neverthless, from lower bounds of $ESN_c^{(K)}$, it is seen that a reasonable performance is obtained even under correlated noise if the DIR length is chosen at an adequate length (3 or 4). From those results, it may be said that noise correlation does not have a serious effect on an SSB-AM system with a data rate of about 10,000 bits/s.

5. Conclusions

We have investigated the performance evaluation of a Viterbi detector under correlated noise. The numerical results showed that noise correlation does not give rise to a serious performance degradation in a communication system with a data rate of about 10,000 bits/s.

Although we made numerical calculations for SSB-AM transmission, QAM (quadrature amplitude modulation) might be employed in a real data communication system. Thus, studies should be done on the correlation noise problem in QAM transmission.

References

1) G. D. Forney, Jr.: IEEE Trans. Inform. Theory, Vol. IT-18 (1972), No. 3, p. 363.
2) S. U. H. Qureshi and E. E. Newhall: IEEE Trans. Inform. Theory, Vol. IT- 19 (1973), No. 4, p. 448.
3) D. D. Falconer and F. R. Magee, Jr.: Bell Syst. Tech. J., Vol. 52 (1973), No. 9, p. 1541.
4) S. A. Fredricsson: IEEE Trans. Inform. Theory, Vol. IT-20 (1974), No. 4, p. 479.
5) S. A. Fredricsson: IEEE Trans. Inform. Theory, Vol. IT-22 (1976), No. 2, p. 200.
6) D. D. Falconer and F. R. Magee, Jr.: IEEE Trans. Commun., Vol. COM-24 (1976), No. 10, p. 1130.
7) D. D. Falconer and F. R. Magee, Jr.: IEEE Trans. Commun., Vol. COM-24 (1976), No. 11, p. 1238.
8) R. E. Bellman: Introduction to Matrix Analysis (1970), McGraw-Hill.
9) U. Grenander and G. Szegö: Toeplitz Forms and Their Application (1958), Univ. of California Press.
10) R. W. Lucky, J. Salz and E. J. Weldon, Jr.: Principles of Data Communication (1968), McGraw-Hill.
11) Y. Ogawa, M. Sengoku and T. Matsumoto: Tech. Rep. of IECE Japan, Vol. CS 77-122 (1977), p. 97.